Open Journal of Fluid Dynamics, **2013, 3, 36-41**
http://dx.doi.org/10.4236/ojfd.2013.32A006 Published Online July 2013 (http://www.scirp.org/journal/ojfd)

Wells Turbine for Wave Energy Conversion

—Improvement of the Performance by Means of Impulse Turbine for Bi-Directional Flow

Shinya Okuhara[1], Manabu Takao[2], Akiyasu Takami[2], Toshiaki Setoguchi[3]
[1]Techno Center, Matsue College of Technology, Matsue, Japan
[2]Department of Mechanical Engineering, Matsue College of Technology, Matsue, Japan
[3]Institute of Ocean Energy, Saga University, Saga, Japan
Email: takao@matsue-ct.jp

Received May 29, 2013; revised June 6, 2013; accepted June 13, 2013

ABSTRACT

Wells turbine has inherent disadvantages in comparison with conventional turbines: relative low efficiency at high flow coefficient and poor starting characteristics. To solve these problems, the authors propose Wells turbine with booster turbine for wave energy conversion, in order to improve the performance in this study. This turbine consists of three parts: a large Wells turbine, a small impulse turbine with fixed guide vanes for oscillating airflow, and a generator. It was conjectured that, by coupling the two axial flow turbines together, pneumatic energy from oscillating airflow is captured by Wells turbine at low flow coefficient and that the impulse turbine gets the energy at high flow coefficient. As the first step of this study on the proposed turbine topology, the performance of turbines under steady flow conditions has been investigated experimentally by model testings. Furthermore, we estimate mean efficiency of the turbine by quasi-steady analysis.

Keywords: Fluid Machinery; Wells Turbine; Impulse Turbine; Wave Energy Conversion; Ocean Engineering

1. Introduction

Several of the wave energy devices being studied under many wave energy programs in the United Kingdom, Japan, Portugal, India and other countries make use of the principle of an oscillating water column (OWC) [1]. In such wave energy devices, a water column which oscillates due to wave motion is used to drive an oscillating air column which is converted into mechanical energy. The energy conversion from the oscillating air column can be achieved by using a self-rectifying air turbine such as Wells turbine which was introduced by Dr. A. A. Wells in 1976 [2-6]. **Figure 1** shows outline of Wells turbine. This turbine rotates in a single direction in oscillating airflow and therefore does not require a system of non-return valves. Furthermore, this turbine is one of the simplest and probably the most economical turbines for wave energy conversion. However, according to previous studies, Wells turbine has inherent disadvantages: low efficiency at high flow coefficient and poor starting characteristics in comparison with conventional turbines because of a severe stall [2-6]. Therefore, although a number of OWC based wave energy plants using Wells turbine have been constructed and tested to date, the total conversion efficiencies of the plants were approximately 15% at the best [7-9]. Moreover, Wells turbine has high noise level and maintenance problem because of high rotational speed.

Recently, in order to develop a high performance self-rectifying air turbine for wave energy conversion, an impulse turbine for bi-directional flow has been proposed by the authors [10-12]. **Figure 2** shows outline of the impulse turbine. There are many reports which describe the performance of the impulse turbine both at starting and running conditions. The experimental results of the model testing show that the efficiency of the impulse turbine is high in a wide range of flow coefficient, though its peak efficiency is almost the same as that of Wells turbine [10-12].

The authors propose Wells turbine with booster turbine in this study. An impulse turbine for bi-directional flow is used as the booster turbine in order to improve the efficiency of Wells turbine at high flow coefficient. This turbine consists of a large Wells turbine, a small impulse turbine and a generator, as shown in **Figure 3**. It was conjectured that by coupling the two turbines together, pneumatic energy from oscillating airflow is captured by

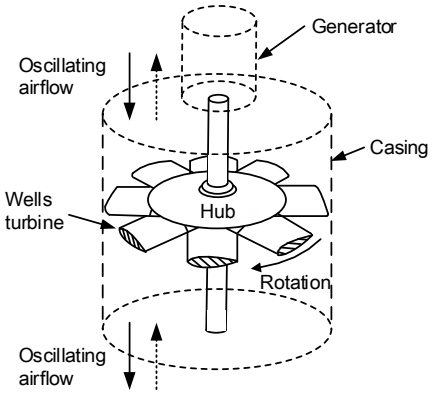

Figure 1. Outline of wells turbine.

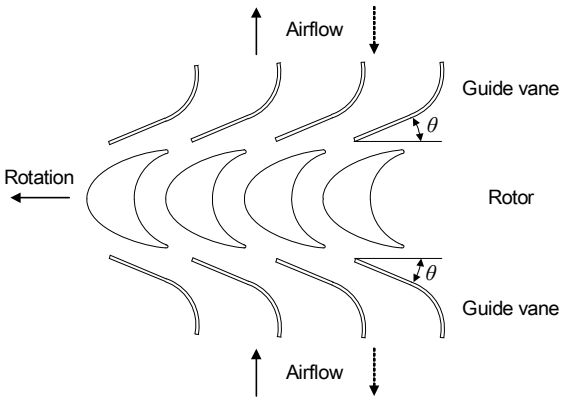

Figure 2. Outline of impulse turbine for wave energy conversion.

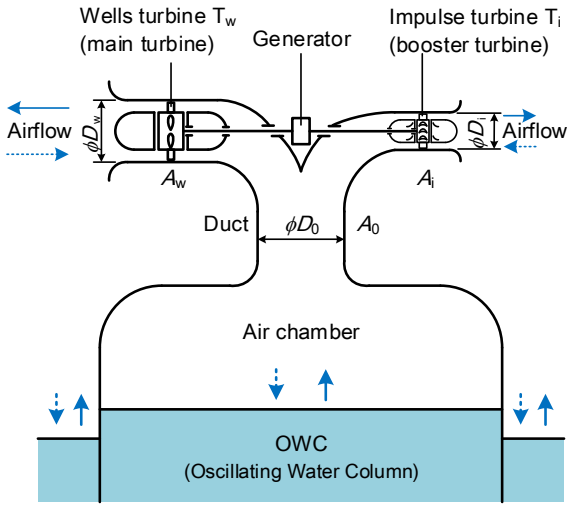

Figure 3. Principle of plant using Wells turbine with booster turbine.

Wells turbine at low flow coefficient and the impulse turbine gets the energy at high flow coefficient. As the first step of study on the proposed turbine topology, the performance of turbines under steady flow conditions have been investigated experimentally by model testing. Further, mean efficiency of the proposed turbine for wave energy conversion has been estimated by quasi-steady analysis in this study.

2. Experimental Apparatus and Procedure

A schematic view of the test rig is shown in **Figure 4**. The test rig consists of a large piston-cylinder (diameter: 1.4 m, length: 1.7 m), one end of which is followed by a settling chamber. Turbine testing is done in 300 mm diameter test section with bell-mouthed entry/exit at both its ends. The piston can be driven back and forth inside the cylinder by means of three ball-screws through three nuts fixed to the piston. All three screws are driven in unison by a D.C. servo-motor through chain and sprockets. A computer controls the motor, and hence the piston velocity to produce any flow velocity. The test turbine is coupled to a servo-motor/generator through a torque transducer. The motor/generator is electrically controlled such that the turbine shaft angular velocity is held constant at any set value. The overall performance was evaluated by the turbine output torque T_o, the flow rate Q, the total pressure drop across the turbine Δp, and the turbine angular velocity ω. The flow rate through the turbine Q, whether it is inhalation (*i.e.*, flow from atmosphere into the settling chamber) or exhalation (*i.e.*, flow from settling chamber to atmosphere), is calculated by measuring the motion of piston, where the value of Q agrees with that obtained by a Pitot tube survey. Tests were performed with the flow rates up to 0.320 m^3/s and the turbine angular velocities up to 471 rad/s. The Reynolds number based on the blade chord was approximately equal to 2.5×10^5 for Wells turbine and 0.5×10^5.

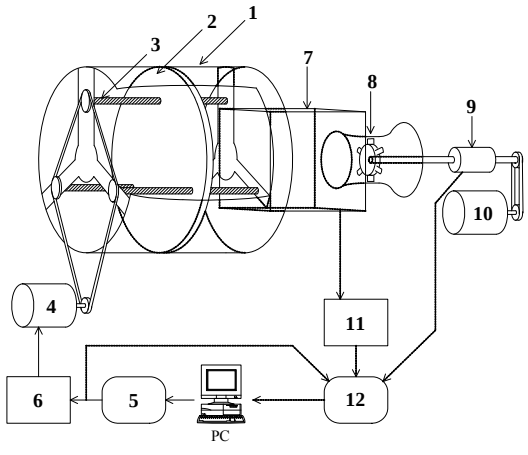

1 Wind tunnel
2 Piston
3 Ball-screw
4 Servomotor
5 D/A converter
6 Servo-pack
7 Settling chamber
8 Turbine
9 Torque transducer
10 Servomotor-generator
11 Pressure transducer
12 A/D converter

Figure 4. Experimental apparatus and measuring system.

The uncertainty of efficiency is about ±1%. This uncertainty has been obtained by taking into account the dispersions in the measurement of the physical parameters from which efficiency is obtained.

3. Tested Axial Turbines

Wells turbine adopted in the experiments is shown in **Figure 5**. The detail of tested Wells turbine in the case of casing diameter D_W = 300 mm is as follows. The chord length, l = 90 mm; blade profile, NACA0020; number of blades, 6; solidity at mean radius, 0.67; hub-to-tip ratio, v = 0.7; aspect ratio, 0.5; tip diameter, 299 mm; tip clearance, 0.5 mm; mean radius, $r_W = D_W(1 + v)/4$ = 127.5 mm; width of flow passage, 45 mm. Note that the adopted turbine rotor is the most promising one in previous studies [3,5,6].

As shown in **Figure 6**, the turbine configuration employed in the study is an impulse type having fixed guide vanes both upstream and downstream, and these geometries are symmetrical with respect to the rotor centerline. The specifications of the impulse turbine rotor in the case of casing diameter D_i = 300 mm are as follows. The rotor blade profile consists of a circular arc on the pressure side and part of an ellipse on the suction side. A radius of the circular is 30.2 mm and the ellipse has semi-major axis of 125.8 mm and semi-minor axis of 41.4 mm. The chord length is 54 mm; solidity of 2.02 at mean radius; blade inlet (or outlet) angle of 60˚; thickness ratio of 0.298; tip diameter of 299 mm; hub-to-tip ratio of v = 0.7; tip clearance of 0.5 mm; mean radius, $r_i = D_i(1 + v)/4$ = 127.5 mm. The guide vane with chord length of 70 mm are symmetrically installed at the distance of 10 mm

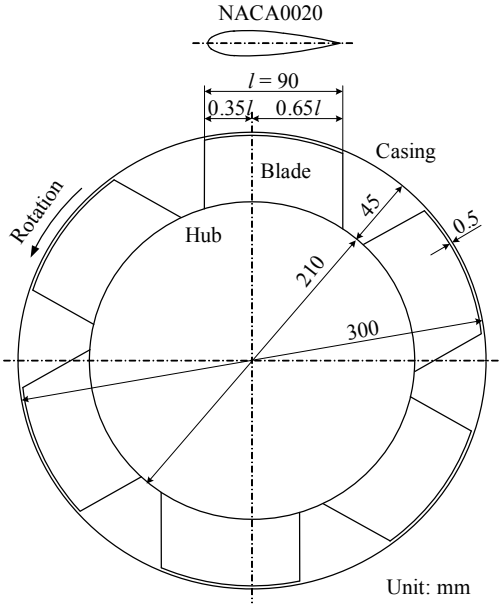

Figure 5. Tested Wells turbine (D_W = 300 mm).

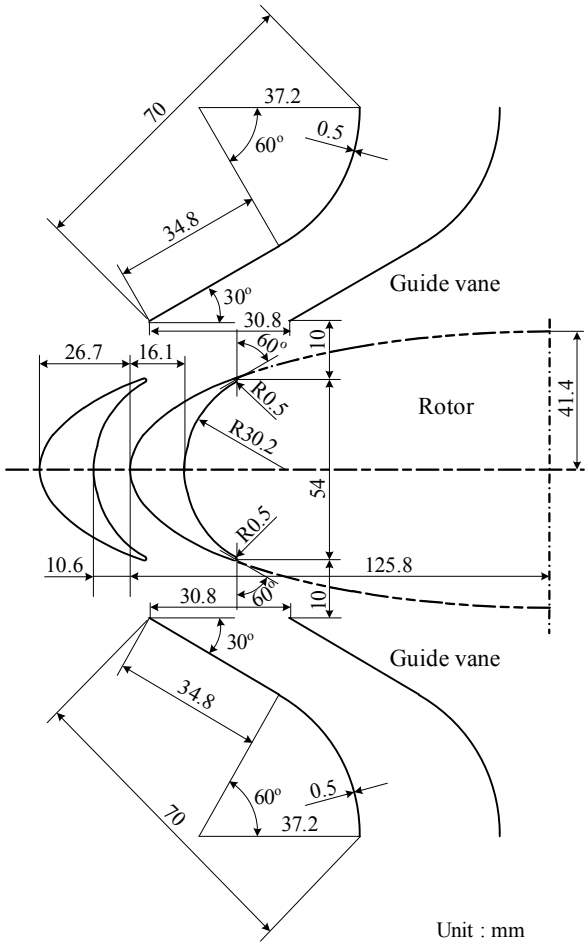

Figure 6. Tested impulse turbine (D_i = 300 mm).

downstream and upstream of the rotor (**Figure 6**). Detailed information about the guide vane is as follows: solidity of 2.27 at mean radius; thickness ratio of 0.0071; a guide vane setting angle of 30˚; camber angle of 60˚. The camber line of guide vane consists of a straight line with a length of 34.8 mm and a circular arc with a radius of 37.2 mm. The rotor blade and guide vane are also the most promising one [10-12].

4. Experimental Results

The turbine performance under steady flow conditions evaluated by turbine efficiency η, torque coefficient C_T and input coefficient C_A against flow coefficient ϕ. The definitions of these parameters are as follows:

$$C_T = T_o \Big/ \left\{ r\left(v^2 + u^2\right) Ar/2 \right\} \tag{1}$$

$$\begin{aligned} C_A &= \Delta pQ \Big/ \left\{ \rho\left(v^2 + u^2\right) Av/2 \right\} \\ &= \Delta p \Big/ \left\{ \rho\left(v^2 + u^2\right)/2 \right\} \end{aligned} \tag{2}$$

$$\eta = T_o \omega / (\Delta pQ) \; = C_T / (C_A \phi) \tag{3}$$

$$\phi = v/u \tag{4}$$

where A, u, v and ρ denote the flow passage area $\left\{=\pi D^2\left(1-\nu^2\right)/4\right\}$, circumferential velocity at mean radius $\{= r\omega\}$, axial flow velocity $\{= Q/A\}$ and density of air, respectively.

Figure 7 shows the experimental results of Wells turbine and the impulse turbine. The torque coefficients C_T of both turbines increase with the flow coefficient ϕ in the region of low flow coefficient (**Figure 7(a)**). However, C_T in the case of Wells turbine drops rapidly at $\phi =$ 0.34 because of stall and it increases with flow coefficient after the stall point again. C_T of the impulse turbine slightly increases in the region of low flow coefficient. However, C_T of the impulse turbine is considerably higher than that of Wells turbine after the stall point of Wells turbine. Similarly, the input coefficients C_A of the turbines also increase ϕ and C_A of Wells turbine slightly decreases at the stall point (**Figure 7(b)**). C_A of the impulse turbine increases with flow coefficient. But C_A of the impulse turbine leveled off after the flow coefficient $\phi = 1.3$. As shown in **Figure 7(c)**, the efficiency of Wells turbine is higher than that of the impulse turbine when ϕ is less than the stall point. But after the stall point of Wells turbine, the efficiency of impulse turbine is considerably higher than that of Wells turbine and the efficiency of Wells turbine is less than 0.04. The peak efficiencies are almost the same and its value is approximately 0.48.

5. Estimation Method of Turbine Characteristics under Sinusoidal Airflow Conditions

Since the airflow into the turbine is generated by the OWC, it is very important to demonstrate the turbine characteristics under oscillating flow conditions. Here let us simulate the characteristics under sinusoidal flow conditions (**Figure 8**) in order to clarify the effect of booster turbine on the efficiency of Wells turbine. The steady flow characteristics of the turbine in **Figures 7(a)** and **(b)** are assumed to be valid for computing performance under unsteady flow conditions. Such a quasi-steady analysis has been validated by previous studies [13,14].

In the calculation, flow rates through the two turbines are obtained by using the steady flow characteristics and solving these simultaneous equations.

$$q = q_W + q_i \tag{5}$$

$$\Delta p_W = \Delta p_i = \Delta p \tag{6}$$

$$\phi_W = v_W/u_W = \left(q_W/A_W\right)/\left(r_W w\right) \tag{7}$$

$$\phi_i = v_i/u_i = \left(q_i/A_i\right)/\left(r_i w\right) \tag{8}$$

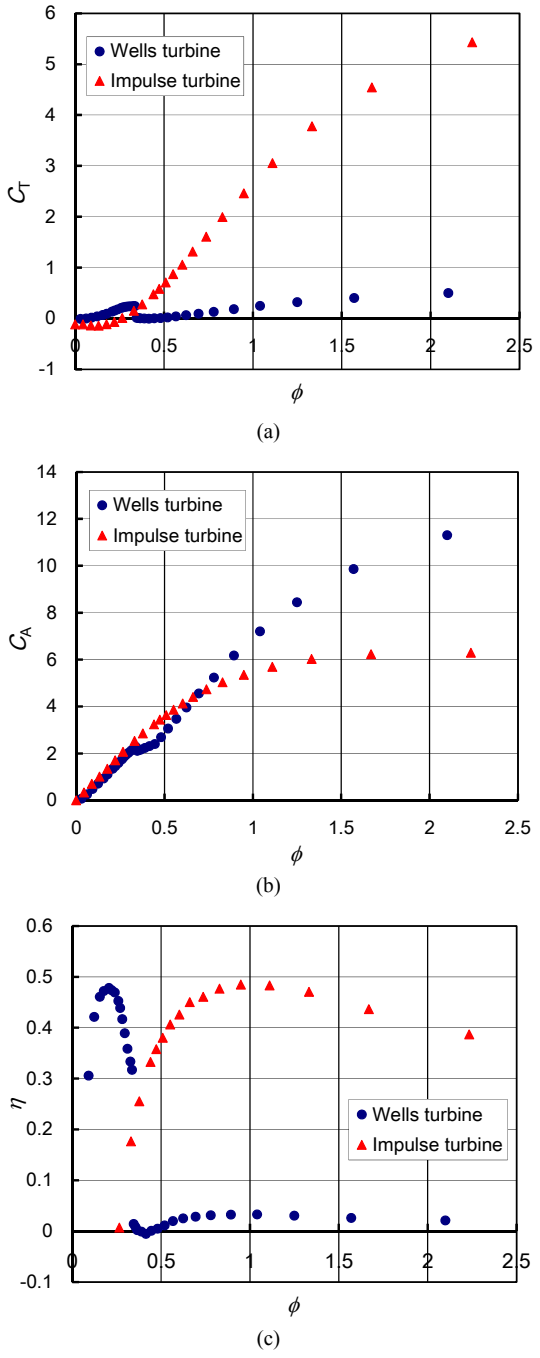

Figure 7. Turbine characteristics under steady flow conditions: (a) Torque coefficient; (b) Input coefficient; (c) Efficiency.

where q denote flow rate through the turbine and subscripts w and i mean Wells turbine T_w and Impulse turbine T_i, respectively (see **Figure 3**). Further, flow rate and rotor angular velocity in the calculations are assumed as follows:

$$q = Q_0 \sin\left(2\pi t/T\right) \tag{9}$$

$$\omega_W = \omega_i = \omega = \text{const.} \tag{10}$$

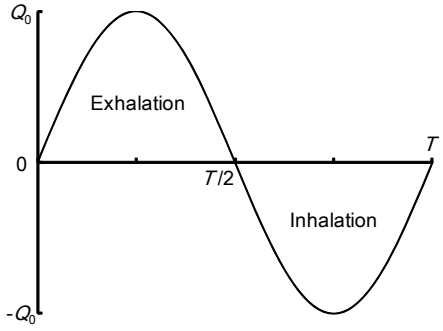

Figure 8. Sinusoidal airflow.

where Q_0, t and T are maximum flow rate, time and period of sinusoidal airflow.

When the turbine is in the running conditions, the parameters such as T_o, ω, Δp and q vary periodically in a sinusoidal oscillating flow. In this case, the turbine performances should be represented by mean value such as mean efficiency. Assuming that only the turbine under forward flow condition operates, in the case of two generators, the running characteristics of the turbine under sinusoidal flow condition are evaluated by mean efficiency η_m against the flow coefficient Φ, which are defined as follows:

$$\Phi = \frac{Q_0/(A_W + A_i)}{(u_W + u_i)/2} \tag{11}$$

The mean efficiency η_m is defined as follows:

$$\eta_m = \frac{\frac{1}{T}\int_0^T (T_{o\,W} + T_{o\,i})\,\omega \mathrm{d}t}{\frac{1}{T}\int_0^T \Delta p q \,\mathrm{d}t} \tag{12}$$

In the study, turbine diameter ratio D_W/D_i changes from 1 to 5 in order to investigate the effect of turbine casing diameters D_W and D_i on mean efficiency. Here, we assumed that total flow passage area of the two turbines equal to area of cross section of the duct in the calculation (See **Figure 3**). That is,

$$\begin{aligned} A_W + A_i &= \pi(1-n^2)\left(\Delta_W^2 + \Delta_i^2\right)/4 \\ &= A_0 = \Delta p Q_0^2/4 \end{aligned} \tag{13}$$

Figures 9 and **10** show the effect of turbine diameter ratio D_W/D_i on mean efficiency η_m and its peak value $\eta_{m,peak}$ under sinusoidal airflow conditions. It is found from the figure that curves of the efficiency have two peaks. The one is at low flow coefficient which is near a flow coefficient of peak efficiency of Wells turbine. Another is at Φ = 1.2 which is near a flow coefficient of peak efficiency of the impulse turbine. The peak mean efficiency decreases with the increase of D_W/D_i when turbine diameter ratio $D_W/D_i \le 1.2$. The peak mean efficiency increase with D_W/D_i when turbine diameter ratio

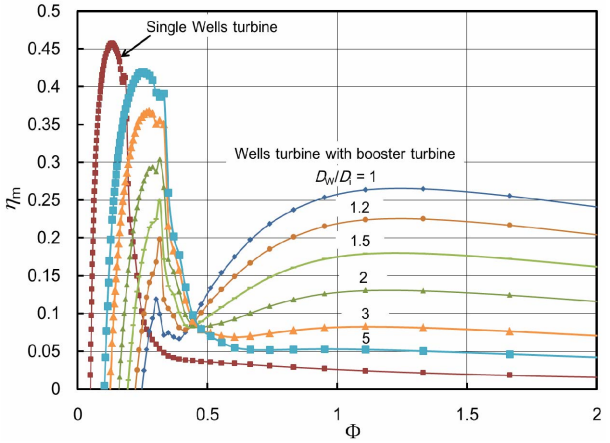

Figure 9. Effect of turbine diameter on mean efficiency under sinusoidal airflow conditions.

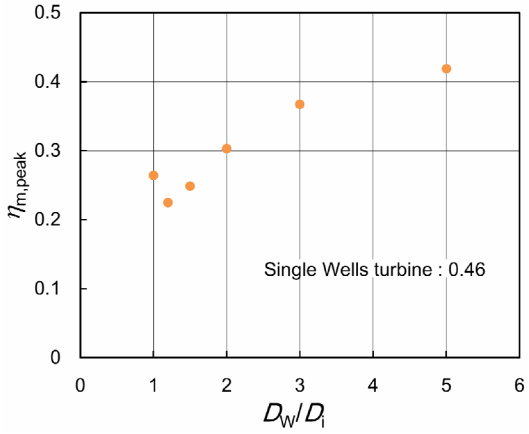

Figure 10. Effect of turbine diameter ratio on mean peak efficiency.

$D_W/D_i > 1.2$. The peak efficiency is lower than that of a single Wells turbine. However, mean efficiency at high flow coefficient in the case of Wells turbine with booster is higher than that of single Wells turbine. It is concluded from this fact that the mean efficiency at high flow coefficient is improved by mean of the impulse turbine as a booster turbine.

6. Conclusions

The authors propose Wells turbine with booster turbine in an OWC configuration in this study, in order to obtain much of wave energy. As the first step of this study, the performances of axial flow turbines under steady flow conditions have been investigated experimentally by model testing. Furthermore, we estimated mean efficiency of the turbine by quasi-steady analysis in this study. The conclusions obtained are summarized as follows.

- The mean efficiency of the turbine strongly depends on turbine diameter ratio.

- The mean efficiency at high flow coefficient is improved by means of the impulse turbine as a booster turbine.
- The peak mean efficiency is lower than that of a single turbine.

REFERENCES

[1] R. Bhattacharyya and M. E. McCormick, "Wave Energy Conversion," Elsevier, Amsterdam, 2003.

[2] T. Setoguchi and M. Takao, "Current Status of Self-Rectifying Air Turbines for Wave Energy Conversion," *Energy Conversion and Management*, Vol. 47, No. 15-16, 2006, pp. 2382-2396. doi:10.1016/j.enconman.2005.11.013

[3] S. Raghunathan, "The Wells Air Turbine for Wave Energy Conversion," *Progress in Aerospace Sciences*, Vol. 31, No. 4, 1995, pp. 335-386. doi:10.1016/0376-0421(95)00001-F

[4] M. Takao, T. Setoguchi, Y. Kinoue, K. Kaneko and S. Nagata, "Improvement of Wells Turbine Performance by Means of End Plate," *Proceedings of the* 16*th International Offshore and Polar Engineering Conference*, San Francisco, 28 May-2 June 2006, pp. 480-484.

[5] K. Kaneko, T. Setoguchi and M. Inoue, "Performance of Wells Turbine in Oscillating Flow," *Proceedings of the Current Practices and New Technology in Ocean Engineering*, *Vol*. 2, American Society of Mechanical Engineers (ASME), New York, 1986, pp. 447-452.

[6] T. Setoguchi, K. Kaneko and M. Inoue, "Determine of Optimum Geometry of Wells Turbine Rotor for Wave Power Generator," *Proceedings of* 3*rd Symposium on Ocean Wave Utilz*, Japan Agency for Marine-Earth Science and Technology (JAMSTEC), Tokyo, 1991, pp. 141-149. (in Japanese)

[7] H. Osawa, Y. Washio, T. Ogata, Y. Tsuritani and Y. Nagata, "The Offshore Floating Type Wave Power Device 'Mighty Whale' Open Sea Tests: Performance of the Prototype," *Proceedings of* 12*th International Offshore and Polar Engineering Conference*, Kitakyushu, 25-31 May 2002, pp. 595-600.

[8] Wavegen, "Islay LIMPET Project Monitoring Final Report," 2002. http://www.wavegen.co.uk/pdf/art.1707.pdf

[9] A. Sarmento, A. Brito-Melo and F. Neumann, "Results from Sea Trials in the OWC European Wave Energy Plant at Pico, Azores," 2006. http://www.pico-owc.net/files/33/cms_b6cda17abb967ed28ec9610137aa45f7.doc

[10] T. Setoguchi, M. Takao, Y. Kinoue, K. Kaneko, S. Santhakumar and M. Inoue, "Study on an Impulse Turbine for Wave Energy Conversion," *International Journal of Offshore and Polar Engineering*, Vol. 10, No. 2, 2000, pp. 145-152.

[11] T. Setoguchi, S. Santhakumar, H. Maeda, M. Takao and K. Kaneko, "A Review of Impulse Turbine for Wave Energy Conversion," *Renewable Energy*, Vol. 23, No. 2, 2001, pp. 261-292. doi:10.1016/S0960-1481(00)00175-0

[12] T. Setoguchi, M. Takao, S. Santhakumar and K. Kaneko, "Study of an Impulse Turbine for Wave Power Conversion: Effects of Reynolds Number and Hub-to-Tip Ratio on Performance," *Journal of Offshore Mechanics and Arctic Engineering*, Vol. 126, No. 2, 2004, pp. 137-140. doi:10.1115/1.1710868

[13] T. Setoguchi, K. Kaneko, H. Maeda, T. W. Kim and M. Inoue, "Impulse Turbine with Self-Pitch-Controlled Guide Vanes for Power Conversion: Performance of Mono-Vane Type," *International Journal of Offshore and Polar Engineering*, Vol. 3, No. 1, 1993, pp. 73-78.

[14] M. Takao, T. Setoguchi, K. Kaneko, T. H. Kim, H. Maeda and M. Inoue, "Impulse Turbine for Wave Power Conversion with Air Flow Rectification System," *International Journal of Offshore and Polar Engineering*, Vol. 12, No. 2, 2002, pp. 142-146.

Nomenclature

A: flow passage area (m^2)
C_A: input coefficient
C_T: torque coefficient
D: casing diameter (m)
l: chord length (m)
q: flow rate under unsteady flow condition (m^3/s)
Q: flow rate under steady flow condition (m^3/s)
Q_0: maximum flow rate of sinusoidal airflow (m^3/s)
r: mean radius (m)
t: time (s)
T: period of sinusoidal airflow (s)
T_o: torque (N-m)
u: circumferential velocity (m/s)
v: axial velocity (m/s)

Greek Letters

Δp: total pressure drop across turbine (Pa)
ϕ: flow coefficient under steady flow condition
Φ: flow coefficient under sinusoidal flow condition
η: efficiency
v: hub-to-tip ratio
ρ: density of air (kg/m^3)
ω: angular velocity (rad/s)

Subscripts

0: duct
W: Wells turbine
i: impulse turbine
m: mean value

